Pergamon

Acta mater. 49 (2001) 3143–3147

Acta MATERIALIA

www.elsevier.com/locate/actamat

SIZE-DEPENDENT INTERFACE ENERGY AND RELATED INTERFACE STRESS

Q. JIANG†, D. S. ZHAO and M. ZHAO

Department of Materials Science and Engineering, Jilin University, Changchun 130025, People's Republic of China

(Received 26 March 2001; received in revised form 30 May 2001; accepted 10 June 2001)

Abstract—General equations for the size-dependence of solid–liquid interface energy, grain boundary energy and the intrinsic interface stress without free parameters are derived. The predicted results correspond to computer simulation results, the first principles calculation, the modified embedded-atom-method potential results and experimental results. In addition, the possible physical background of positive or negative interface stress is analyzed.

Keywords: Size-dependence; Interface

1. INTRODUCTION

For nanophases and nanostructured materials, surface (interface) excess Gibbs free energy γ and related surface (interface) stress f determine their thermal stability due to their large surface/volume ratio. γ describes the reversible work per unit area to form a new solid surface while f being the derivative of γ with respect to the strain tangentia1 to the surface denotes the reversible work per unit area due to elastic deformation [1–3]. Note that f here refers to intrinsic stress that is not the result of directly applied loads or of differential thermal expansion. Both γ and f are fundamental thermodynamic quantities where few reliable experimental or theoretical values are available [1–3]. Therefore, the derivation of their general expressions without free parameters would have general curiosity and importance for nanophases and nanostructured materials.

Although Langmuir has considered the temperature dependence of the solid–vapor interface energy $\gamma_{sv}(T)$ in 1916 where T denotes temperature [4], the size-dependence of $\gamma_{sv}(D)$ was thermodynamically considered [5–7] thirty years later with the following form [7]

$$\gamma_{sv}(D)/\gamma_{sv0} = 1-4h/D + \ldots, \quad (1)$$

where γ_{sv0} is the corresponding bulk value of $\gamma_{sv}(D)$, h denotes atomic diameter and D denotes the particle diameter. According to the quantum chemistry consideration, the above equation could be valid even if the size of a particle is as small as a cluster having several atoms [8]. For the size-dependence of solid–liquid interface energy $\gamma_{sl}(D)$ and solid–solid interface energy $\gamma_{ss}(D)$, a similar form has been deduced later although the coefficient of $1/D$ term is unknown [8].

In equation (1), value of γ_{sv0} of metallic elements has been calculated by computer simulation [9]. However, a general equation for the γ_{sv0} value is still lacking [9]. On the other side, simple thermodynamic equations for bulk solid–liquid interface energy γ_{sl0} [10] and bulk solid–solid interface energy or grain boundary energy γ_{ss0} [11] have been obtained. For γ_{sl0}, it reads [10]

$$\gamma_{sl0} = 2hS_{vib}H_m(T)/(3V_mR), \quad (2)$$

with R being the ideal gas constant, $H_m(T)$ being the temperature-dependent melting enthalpy of crystals, S_{vib} the vibrational part of the overall melting entropy S_m and V_m the molar volume of crystals. Although S_m consists, at least, of three contributions: positional S_{pos}, vibrational S_{vib} and electronic component S_{el} [12, 13], if the type of chemical connection does not vary at transition, electronic component is neglectfully small. S_{pos} is apparently also small for metallic and organic crystals. Thus, S_m for metallic and organic crystals is mainly vibrational in nature and $S_{vib} \approx S_m$ is used [12]. However, for a semiconductor crystal, melting is accompanied by a semiconductor-to-metal transition, S_{el} should strongly contribute to S_m.

† To whom all correspondence should be addressed. Tel.: +86-431-570-5371; fax: +86-431-568-7607.

E-mail address: jiangq@jlu.edu.cn (Q. Jiang)

1359-6454/01/$20.00
PII: S1359-6454(01)00232-4

In equation (2), $H_m(T) = g_m(T) - T\mathrm{d}g_m(T)/\mathrm{d}T$ (Helmholtz function) where $g_m(T)$ is the temperature-dependent solid–liquid Gibbs free energy difference. For metallic elements, $g_m(T) = H_m(T_m - T)(7T)/[T_m(T_m + 6T)]$ where H_m is the melting enthalpy at the melting temperature T_m [14, 15]. With the $g_m(T)$ function, $H_m(T) = 49T^2H_m/(T_m + 6T)^2$. Now, equation (2) can be rewritten as

$$\gamma_{sl0} = \frac{98hT^2H_mS_{vib}}{3R(T_m + 6T)^2V_m}. \tag{3}$$

According to the relationship of $\gamma_{ss0} \approx 2\gamma_{sl0}$ [16] and equation (3)

$$\gamma_{ss0} = \frac{196hT^2H_mS_{vib}}{3R(T_m + 6T)^2V_m}. \tag{4}$$

In fact, equation (4) is the same of the phenomenological equation of $1.3hH_m/V_m$ [11] under the assumption that $S_{vib}/R \approx 1$, $T = T_m$ and $1.3 \approx 4/3$.

For f, there is no such kind of equation up to now although many theoretical approaches and experiments with discrepancy have been carried out [1–3, 17–21].

In this contribution, based on the above results for the interface energy and the corresponding size-dependence, we develop thermodynamic equations that suggest $\gamma_{sl}(D)$ and $\gamma_{ss}(D)$ functions and the related expression for f. The predicted results are in agreement with other theoretical results and experimental evidences.

2. MODEL

To determine a $\gamma_{sl}(D)$ function, we consider a compressible spherical particle with a diameter D, or a cube with cube side taken as D, immersed in the corresponding bulk liquid. According to the Laplace–Young equation [2], we have

$$P = 2fA/(3V) = 4f/D, \tag{5}$$

where A and V are the surface area and the volume of the particle and P the difference in pressure inside and outside of the particle. Using the definition of compressibility $\kappa = -\Delta V/(VP)$, $\epsilon = \Delta D/D = \Delta A/(2A) = \Delta V/(3V)$ under small strain and $A/V = 6/D$ where Δ denotes the difference

$$\epsilon = -4\kappa f/(3D). \tag{6}$$

In terms of a scalar definition of f, there exists [1–3]

$$f = \partial G/\partial A = \partial(\gamma_{sl}A)/\partial A = \gamma_{sl} + A\partial\gamma_{sl}/\partial A \approx \gamma_{sl} + A\Delta\gamma_{sl}/\Delta A \tag{7}$$

where $G = \gamma_{sl}A$ states the total excess Gibbs surface free energy, or

$$\Delta\gamma_{sl} = (\Delta A/A)(f - \gamma_{sl}). \tag{8}$$

To find mathematical solutions of f and γ_{sl} or $\gamma_{sl}(D)$, two boundary conditions of $\gamma_{sl}(D)$ are needed. An understandable asymptotic limit is that as $D \to \infty$, $\gamma_{sl}(D) \to \gamma_{sl0}$. As $D \to \infty$, let

$$\Delta\gamma_{sl} = \gamma_{sl}(D) - \gamma_{sl0}. \tag{9}$$

Substituting equation (9) into equation (8) and taking in mind that $V/A = D/6$ and $\Delta A/A = 2\epsilon = -8\kappa f/(3D)$ in terms of equation (6)

$$\gamma_{sl}(D)/\gamma_{sl0} = [1 - 8\kappa f^2/(3\gamma_{sl0}D)]/[1 - 8\kappa f/(3D)]. \tag{10}$$

Equation (10) is consistent with general calculations of thermodynamics [17, 21, 22] and quantum chemistry [8] for particles in a similar form of equation (1). Note that since f is one order larger than γ_{sl0} as seen in Table 1, the effect of the denominator in equation (10) on $\gamma_{sl}(D)$ value is minor.

To determine f, we assume that when almost all atoms of a low-dimensional crystal immersed in fluid is located on its surface with a diameter of D_0, the crystal is indistinguishable from the surrounding fluid where the solid–liquid interface is at all diffuse. Note that the crystal is now similar to a cluster produced by an energetic fluctuation of the fluid. This assumption leads to a limit case: as $D \to D_0$, $\gamma_{sl} \to 0$ where D_0 depends on the existence of curvature [20]. Let d denote the dimension of a low-dimensional crystal, for a particle (d=0) or a wire (d=1), D has a usual meaning of diameter (if the particle or the wire is cubic or rhombohedral, D is defined as the side length) [12]. For a film (d=2), D denotes its thickness [12]. Note that when a crystal has plane surface, such as a film, the possible smallest value of D is $2h$. For any crystals with curved surfaces, such as a particle or a wire, the possible smallest D is $3h$. According to the above definition of D_0, $hA/V = 1 - V_i/V = 1 - [(D_0 - 2h)/D_0]^{3-d} = 1$ where V_i is the interior volume of the crystal. The solution of the above equation is $D_0 = 2h$. For the particle and the wire usually having a curved surface, D values cannot be smaller than $3h$. In this case, there is no exact solution of the equation. As a first order approximation, $D_0 = 3h$ is taken. Note that this approximation does not lead to big error. For instance, for a spherical particle, $hA/V = 26/27 \approx 1$. In summary

$$D_0 = 3h, \tag{11a}$$

$$D_0 = 2h \tag{11b}$$

Table 1. Comparison of surface stress among our model prediction, experimental results and other theoretical results for some metallic elements with corresponding thermal parameters. h values come from Ref. [24], V_m, H_m and T_m values are cited from Ref. [25], $S_{vib}\approx S_m=H_m/T_m$, and $\kappa=1/B$ where B is the bulk modulus cited from Ref. [26]. γ_{sl0} and γ_{ss0} are calculated in terms of equations (3) and (4) at T_k where T_k determined by $dg_m(T)/dT=0$ is the ideal glass transition temperature or the isentropic temperature. f_1 is determined in terms of equation (13) with $D_0=2h$ for the case of thin film at T_k. Note that the temperature-dependence of $H_m(T)$ is induced by the difference of specific heat between the crystal and the liquid ΔC_p. At $T<T_k$, liquid transforms to glass and ΔC_p between the crystal and glass could be neglected [14,15] and $H_m(T<T_k)\approx H_m(T_k)$. Therefore, $f_1(T_k)\approx f_1(0)$. f_2 denotes the results of the first principles calculation at 0 K [1], f_3 shows the computer simulation results at 0 K [17] and f_4 denotes the results of the modified embedded atom method potentials at 0 K [18]. f_5 shows the experimental results at 323, 338, 328 K for Au, Pt and Ag, respectively [1]

	Au	Pt	Ag	Cu	Ni	Al	Pb	Ir
h (nm)	0.2884	0.2775	0.2889	0.2556	0.2492	0.2863	0.3500	0.2174
V_m ($cm^3\ mol^{-1}$)	10.2	9.1	10.3	7.1	6.59	10	18.17	8.54
H_m ($kJ\ mol^{-1}$)	12.55	19.6	11.3	13.05	17.47	10.79	4.799	26.1
T_m (K)	1337.6	2045	1234	1357.6	1726	933.25	600.6	2716
S_m ($J\ mol^{-1}K^{-1}$)	9.38	9.58	9.16	9.61	10.12	11.56	7.99	9.61
κ ($10^{-12}\ Pa^{-1}$)	5.8480	3.6232	9.6525	7.2569	5.6402	13.298	21.834	2.6954
γ_{sl0} (J/m^2)	0.139	0.239	0.121	0.188	0.279	0.149	0.031	0.266
γ_{ss0} (J/m^2)	0.278	0.478	0.242	0.376	0.558	0.298	0.062	0.532
f_1 (J/m^2)	2.27	3.71	1.65	2.23	3.04	1.55	0.61	4.01
f_2 (J/m^2)	2.77	5.60				1.25	0.82	5.30
f_3 (J/m^2)	1.714		1.041	1.106	0.817			
f_4 (J/m^2)			1.94		1.67			
f_5 (J/m^2)	1.175±0.2	2.574±0.4	1.415±0.3					

where equation (11a) for a particle or a wire with a curved surface and equation (11b) for a film with a plane surface. Now equation (10) can be rewritten as

$$\gamma_{sl}(D)/\gamma_{sl0} = [1-D_0/D]/[1-\gamma_{sl0}D_0/(fD)] \quad (12)$$

with $8\kappa f^2/(3\gamma_0) = D_0$, or

$$f = \pm[(3\gamma_{sl0}D_0)/(8\kappa)]^{1/2}. \quad (13)$$

Note that under the conditions of $\gamma_{sl}(D_0) = 0$ and $0\le\gamma_{sl}(D)/\gamma_{sl0}\le 1$, f has only two, but not three roots from equation (12).

For solid–solid interface or grain boundary, the above equations must be modified due to different interface conditions. We assume that f as a first order approximation keeps constant for both of solid–liquid and solid–solid interface, which leads to the same strain on both sides of the interface when the grains are isotropic. However, elastic modulus of grain boundaries should be larger than that of the solid–liquid interface with less strain under the same stress. This is introduced by the fact that $A = 3V/D$ for solid–solid interface because two solid–liquid interfaces of particles combine to form one grain boundary with

$$P = 2fA/(3V) = 2f/D, \quad (14)$$

and

$$\epsilon = -2\kappa f/(3D). \quad (15)$$

Equation (15) indicates that the strain on the grain boundary is only a half of that on the solid–liquid interface and thus $\Delta A/A = 2\epsilon = -4\kappa(3D)$. Now $\Delta\gamma_{ss} = \gamma_{ss}-\gamma_{ss0} = (\Delta A/A)(f-\gamma_{ss}) = -4\kappa f/(3D)(f-\gamma_{ss})$, or

$$\gamma_{ss}(D)/\gamma_{ss0} = [1-4\kappa f^2/(3\gamma_{ss0}D)]/[1-4\kappa f/(3D)] = [1-D_0/(4D)]/[1-\gamma_{ss0}D_0/(4fD)]. \quad (16)$$

Equation (16) clearly shows that the size-dependence of $\gamma_{ss}(D)$ function is weaker than that of $\gamma_{sl}(D)$ function due to the strong effect of relevant grains on strains.

3. RESULTS

Figure 1 compares the model prediction of equations (12) and (16) and computer simulation results of $\gamma_{sl}(D)$ and $\gamma_{ss}(D)$ functions [22, 23]. It is evident that the model predictions are consistent with the

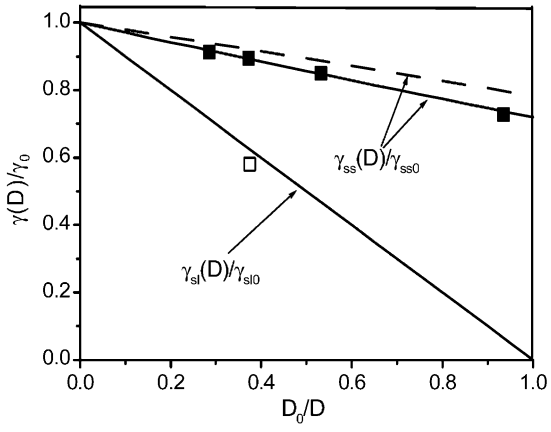

Fig. 1. $\gamma(D)/\gamma_0$ as a function of D_0/D according to equations (12) and (16). For $\gamma_{ss}(D)/\gamma_{ss0}$ function, the solid line and the segment line are obtained by use of negative and positive f, respectively. The open square denotes the computer simulation result of $\gamma_{sl}(8h)$ and $\gamma_{sl}(8h)/\gamma_{sl0} = 0.58$ [22]. The solid squares denote the computer simulation results of Cu where γ_{ss0}=0.733 J/m^2 [23]. $D_0 = 3h$ in terms of equation (11a).

computer simulation results: $\gamma_{sl}(D)$ and $\gamma_{ss}(D)$ values reduce as D decreases but with different dropping tendencies. In Fig. 1, since an unknown fcc crystal of solid–liquid interface energy is cited [22], we use the simplified form of equation (12) of $\gamma_{sl}(D)/\gamma_{sl0} = [1-D_0/D]$ with neglecting the factor of $1/[1-\gamma_{sl0}D_0/(fD)]$, which results in minor error as stated above. It is interesting that the use of a negative interface stress for $\gamma_{ss}(D)$ in equation (16) leads to a full agreement with the computer simulation results, which implies that $f<0$.

If we compare equations (1), (12) and (16), we found that $\gamma_{sv}(D)/\gamma_{sv0}<\gamma_{sl}(D)/\gamma_{sl0}<\gamma_{ss}(D)/\gamma_{ss0}$ which implies that the stiffer surrounding of particles brings out less decrease of the interface energy as D minimizes. For the grain boundaries, even if when $D\rightarrow D_0$, $\gamma_{ss}(D)/\gamma_{ss0}\approx 75\%$. Since when $D\approx 2D_0$, the grains are no more stable and will transform to amorphous solids in terms of the computer simulation results [23], the smallest value of $\gamma_{ss}(2D_0)/\gamma_{ss0}$ could be about 85%.

The above consistence for $\gamma_{sl}(D)$ and $\gamma_{ss}(D)$ functions between the model predictions and the computer simulation results in return confirms that equation (13) for f is also reasonable. This correspondence can be observed in Tables 1 and 2 where the calculated f values for metallic single crystals and multi-layer films in terms of equation (13) and the corresponding experimental and theoretical results are also shown. In the comparison, we have assumed that our estimation of f is also applicable not only for solid–liquid and solid–solid interfaces, but also for solid–vapor interfaces. Note that positive values of f are used for single elements while negative values of f are given for the multilayers consisting of different metallic elements although other theoretical works cannot indicate negative interface stress [20]. Our results are in agreement with the theoretical works [1] and the experimental results [1, 3] in error range.

The possible physical background of the positive or negative f could be analyzed in the following way. When the interface atoms suffer a coordination number (CN) or bond strength (σ) decrease, bond contraction of interface atoms arises [27], which could lead to a positive f. This is the case of nanoparticles. When the interface atoms are exposed to CN or σ increase, such as multilayers with different elements while the element with lower melting temperature has lower σ within the layer than that on the interface, bond expansion of interface atoms is present, which should result in negative f [28]. For nanostructured materials, the situation is more complicated. When the nanostructured materials consist of different phases, there could be a similar case of multilayers. If the nanostructured materials consist of a single phase, σ of interface atoms and that within the grain should be same. As the CN of the atoms on the interface is larger or smaller than that within the grain, both bond expansion or bond extraction as well as corresponding negative or positive f could be present. In fact, the consideration about the bond strength increase of atoms on the interface has successfully interpreted the melting temperature and melting entropy increase of nanoparticles embedded in a matrix [29].

Table 2. The comparison of f in J/m^2 for incoherent multilayers between our model and experimental results. As the first order approximation, values of γ_{sl0} and κ on the layer interface are considered as algebra average values of two elements where γ_{sl0} and κ values of each element see Table 1. The experimental results come from Ref. [3]

Multi-layer A/B	Our calculations	Experimental results
Ag/Ni	−2.297	−2.27±0.67, −2.24±0.21, −2.02±0.26
Ag/Cu	−1.932	−3.19±0.43, −0.21±0.10

4. CONCLUSIONS

In summary, we have established general models for size-dependence, temperature-dependence and curvature-dependence of solid–liquid and solid–solid interface energies as well as corresponding interface stress. The agreement among our estimation, the other theoretical works and the experimental results has been found. Moreover, the reason for different signs of interface stress under different conditions has been analyzed.

Acknowledgements—Financial support from the NNSFC under Grant No. 59931030, 50071023, 50025101 and from the Trans-Century Training Program Foundation for the Talents by the Ministry of Education of China is acknowledged.

REFERENCES

1. Cammarata, R. C. and Sieradzki, K., *Annu. Rev. Mater. Sci.*, 1994, **24**, 215, (and reference therein).
2. Weissmüller, J. and Cahn, J. W., *Acta mater.*, 1997, **45**, 1899.
3. Spaepen, F., *Acta mater.*, 2000, **48**, 31, (and reference therein).
4. Langmuir, I., *J. Am. Chem. Soc.*, 1916, **38**, 2221.
5. Tolman, R. C., *J. Chem. Phys.*, 1949, **17**, 333.
6. Kirkwood, J. G. and Buff, F. P., *J. Chem. Phys.*, 1949, **17**, 338.
7. Buff, F. P., *J. Chem. Phys.*, 1951, **19**, 1591.
8. Müller, H., Opitz, Ch., Strickert, K. and Skala, L., *Z. Phys. Chemie Leipzig*, 1987, **268**, 625.
9. Vitos, L., Ruban, A. V., Skriver, H. L. and Kollar, J., *Surf. Sci.*, 1998, **411**, 186.
10. Jiang, Q., Shi, H. X. and Zhao, M., *Acta mater.*, 1999, **47**, 2109.
11. Weissmüller, J., *Nanostructured Mater.*, 1993, **3**, 261.
12. Jiang, Q., Shi, H. X. and Zhao, M., *J. Chem. Phys.*, 1999, **111**, 2176.
13. Regel, A. R. and Glazov, V. M., *Semiconductors*, 1995, **29**, 405.
14. Singh, H. B. and Holz, A., *Solid State Commun.*, 1983, **45**, 985.
15. Perepezko, J. H. and Palk, J. S., *J. Non-Cryst. Solids*, 1984, **61 and 62**, 113.
16. Kotze, I. A. and Kuhlmann-Wilsdorf, D., *Appl. Phys. Lett.*, 1966, **9**, 96.
17. Streitz, F. H., Cammarata, R. C. and Sieradzki, K., *Phys. Rev. B*, 1994, **49**, 10699.
18. Streitz, F. H., Cammarata, R. C. and Sieradzki, K., *Phys. Rev. B*, 1994, **49**, 10707.

19. Weissmüller, J., in *Nanomaterials: Systhesis, Properties and Applications*, ed. A. S. Edelstein and R. C. Cammarata. Institute of Physics Publishing, Bristol and Philadelphia, 1996, p. 219.
20. Nix, W. D. and Gao, H., *Scripta mater.*, 1998, **39**, 1653.
21. Cammarata, R. C., Sieradzki, K. and Spaepen, F., *J. Appl. Phys.*, 2000, **87**, 1227.
22. Broughton, J. Q. and Glimer, G. H., *J. Chem. Phys.*, 1986, **84**, 5759.
23. Wang, J., Wolf, D., Philpot, S. R. and Gleiter, H., *Philos. Mag. A*, 1996, **73**, 517.
24. King, H. W., in *Physical Metallurgy*, ed. R. W. Cahn. North-Holland, Amsterdam, 1970, p. 60.
25. Sargent Welch scientific company, *Table of Periodic Properties of the Elements*. Skokie, Illinois, 1980, p. 1.
26. Brandes, E. A. (ed.), *Smithells Metals Reference Book*, 6th ed. Butterworth, London 1983, p. 15.
27. Sun, C. Q., *J. Phys.: Condens. Mater.*, 1999, **11**, 4801.
28. Nanda, K. K., Behera, S. N. and Sahu, S. N., *J. Phys.: Condens. Mater.*, 2001, **13**, 2861.
29. Jiang, Q., Zhang, Z. and Li, J. C., *Acta mater.*, 2000, **48**, 4791.